The role of ion kinetic Kelvin-Helmholtz and interchange instabilities in edge plasma blob formation

P W Gingell[1], S C Chapman[2,3] and R O Dendy[2,4]

[1]*School of Physics and Astronomy, Queen Mary, University of London 327 Mile End Road, London, E1 4NS UK*

[2]*Centre for Fusion, Space and Astrophysics, Department of Physics, Warwick University, Coventry CV4 7AL, UK*

[3]*Department of Mathematics and Statistics, Tromsø University, N-9037 Tromsø, Norway*

[4]*CCFE, Culham Science Centre, Abingdon, Oxfordshire OX14 3DB, U.K.*

1. Introduction

Radially propagating, coherent filamentary structures (which appear as "blobs" in poloidal projection) are observed in the near-edge region of tokamak plasmas. These grow from turbulence[1,2] excited by the drift and interchange instabilities at the outboard side of the torus, driven by magnetic curvature and pressure gradients perpendicular to the magnetic field. Propagating[3] blobs are fluctuations of density, electron temperature and potential with amplitudes[4] of order 5%–100% of the background values, with smaller fluctuations in the magnetic field. Blob populations have been reported for several tokamaks[5–9], and may account for up to 50% of particle transport across the scrape-off layer (SOL) towards the vessel wall[5], with implications for future large tokamak plasmas[10]. The distribution of blob sizes is likely to include a population with radii comparable to the ion gyroradius, which is unresolvable by existing diagnostic observations. Here we report recent large scale numerical simulations[11] which use a hybrid model (kinetic ions, fluid electrons) to study mechanisms for the creation of ion gyro-scale blobs. This level of description captures ion kinetic physics that cannot be retained by multi-fluid models. The primary mechanisms for blob generation investigated here are thus the ion kinetic generalisations of the Kelvin-Helmholtz and interchange instabilities. We present statistics of the sizes of blobs created by these instabilities, together with radial particle displacement data. We find that ion gyro-scale blobs constitute a significant portion of the blob population, and that for larger ion gyro-radii there is an increase in radial transport. Results are compared for pure proton plasmas and for a 50:50 deuterium-tritium mix, relevant to burning plasmas. The dynamics of ion gyroscale blobs are understood[12], and they can contribute disproportionately well to plasma heating[13]. Having now investigated blob generation[11], we conclude that ion kinetic physics plays a significant role in the transport of energy and particles by ion gyro-scale blobs in the low-field near-edge region of tokamak plasmas.

2. Computational model and simulation scenarios

The hybrid description treats ions kinetically. Their trajectories in the full six-dimensional phase space result from the Lorentz force due to three-dimensional (3D) vector $\boldsymbol{E}$ and $\boldsymbol{B}$ fields. Electromagnetic fields are evolved self-consistently with

the kinetic ions and fluid electrons, using Maxwell's equations and Ohm's law in the low frequency limit. The model assumptions are: inertia-less electrons; electric field divergence negligible on the lengthscales of interest, implying charge neutrality; collisionless plasma; and an ideal, isothermal electron fluid. The full 3D $\boldsymbol{E}$, $\boldsymbol{B}$ and $\boldsymbol{J}$ vector fields are advanced with second-order accuracy on a two-dimensional (2D) grid in space (x,y) and in time. Particle positions are updated in 2D in configuration space and 3D in velocity space. We refer to Refs.[11-13] for further details.

In our simulations, background parameters are representative of conditions towards the edge of a low-field tokamak: $n_0 = 10^{19}\mathrm{m}^{-3}$, $T_\mathrm{i} = T_\mathrm{e} = 4 \times 10^6\mathrm{K}$, $B_0 = 0.4\mathrm{T}$, see further table 1 of Ref.[11]. Differing initial conditions are applied, which lead to the growth of the interchange or Kelvin-Helmholtz instabilities separately and in combination, for proton plasmas and for a 50:50 deuterium-tritium mix. We simulate a boundary region internal to the plasma. A density gradient is set up at $y = 0$, with width a and maximum and minimum densities $n_\mathrm{bot} = 4n_0$ and $n_\mathrm{top} = n_0$ respectively; this initialises the simulation with a pressure gradient to drive the interchange instability. Some simulations also include a velocity shear boundary at $y = 0$, with $u_\mathrm{bot} = -0.02v_\mathrm{A}$ and $u_\mathrm{top} = 0.02v_\mathrm{A}$, where v_A denotes the Alfvén velocity. The initial width a of both the density gradient and shear boundary is equal to the cell size Δx. The plasma is initially homogeneous in the (x,y) plane in both temperature and magnetic field. The background magnetic field $\boldsymbol{B}_0 = (0,0,B_0)$ is initialised perpendicular to both the plane of the simulation and the background flows, so there is no magnetic shear present in the initial conditions. For the simulations reported here, fluctuations in B_z grow with maximum amplitude on the order of 1% of the background field. Given the 2D3V simulation geometry, there are no gradients of the $\boldsymbol{B}$ field in the z-direction. Figure 1 shows a diagram of this geometry.

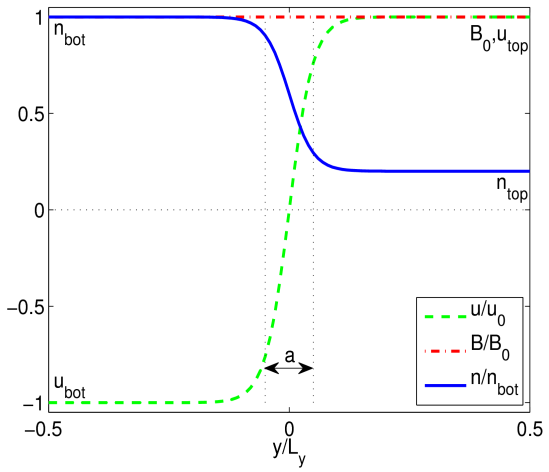

Fig.1 Initial conditions for the simulations. The initial flow velocities $u_\mathrm{top,bot}$ are directed in the $\pm x$ directions, parallel to the boundary layer. The background magnetic field B_0 is in the z direction, perpendicular to the plane of the simulation domain and the background flows.
Reproduced from [11].

3. Simulation results and conclusions

Figure 2 shows the time evolution of the number density of a simulation of a proton plasma with $n_\mathrm{top} = n_0$, $n_\mathrm{bot} = 4n_0$ and $u_\mathrm{top/bot} = 0$. Separation of populations of ions from their initial populations involves fingers of high-density plasma penetrating the $y > 0$ region which is initially occupied by low-density plasma. These finger-like structures, which have scale lengths on the order of the boundary width, are on spatio-temporal scales characteristic of the interchange instability. As seen in figure 2, perturbations at the boundary layer extend in the y-direction from $122t_\Omega$, where t_Ω denotes the

background proton gyroperiod. Separation of blob-like, coherent structures from the fingers begins at approximately $180t_\Omega$, while holes of low density plasma arise in the $y < 0$ region. These structures propagate in the $\pm y$ direction by virtue of the velocity imparted to these populations by the interchange instability. Hence we conclude that the interchange instability can lead to the formation of radially propagating blobs in the plasma region adjacent to the density interface. The amplitude of magnetic fluctuations is less than 1% of the background field over the full simulation domain, and we do not observe changing magnetic topology via reconnection. Our simulations thus demonstrate that it is not necessary for magnetic reconnection to occur, in order for blob detachment to take place, once ion kinetics are fully incorporated in the physical model. For tokamak edge plasmas, density blob detachment does not need to incorporate magnetic flux tube detachment by reconnection of magnetic surfaces.

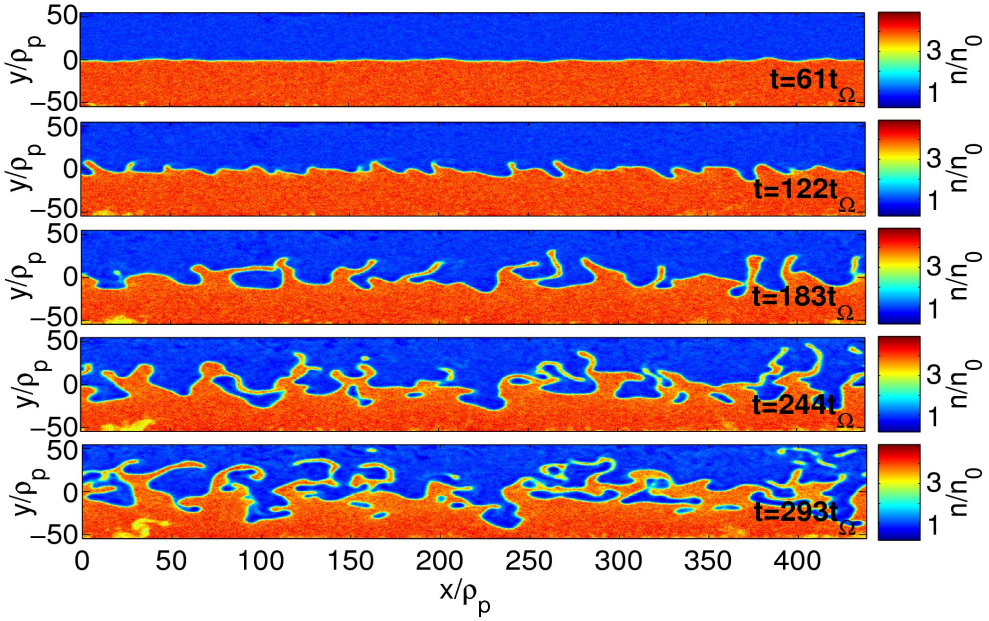

Fig.2 Total number density of ions for a simulation initialized with a pressure gradient of width $a = \Delta y$ at $y = 0$, and $n_{bot} = 4n_{top}$. Perturbations on the boundary layer, visible from $t = 61t_\Omega$, grow at later times due to the interchange instability. Separation of blobs from the higher density layer begins near $t = 200t_\Omega$. Reproduced from [11].

Figure 3 shows cases where the initial conditions include a velocity shear boundary at $y = 0$ with $u_{top/bot} = \pm 0.02v_A$. Here both the interchange and Kelvin-Helmholtz (K-H) instabilities are active. From $60t_\Omega$ in the proton plasma case (left panels) and $20t_\Omega$ in the D-T plasma case (right panels), we see the formation and growth of vortices along the boundary layer with growth rate inversely proportional to the scale size,characteristic of the K-H instability. In both cases, separation of blobs occurs at the crests of the vortices generated by the K-H instability, and at earlier times relative to the simulation with zero velocity shear (figure 2). In the D-T plasma, the growth rate of both K–H and interchange instabilities is significantly reduced compared with the proton plasma case, with suppression of small-scale modes. As a consequence, separation of blobs occurs at later times.

Analysis[11] of the distribution of sizes of blobs created by these instabilities shows that, for ion gyro-scale boundary widths, ion gyro-scale blobs can account for up to 70% of the blob population. A velocity shear boundary can increase the proportion of

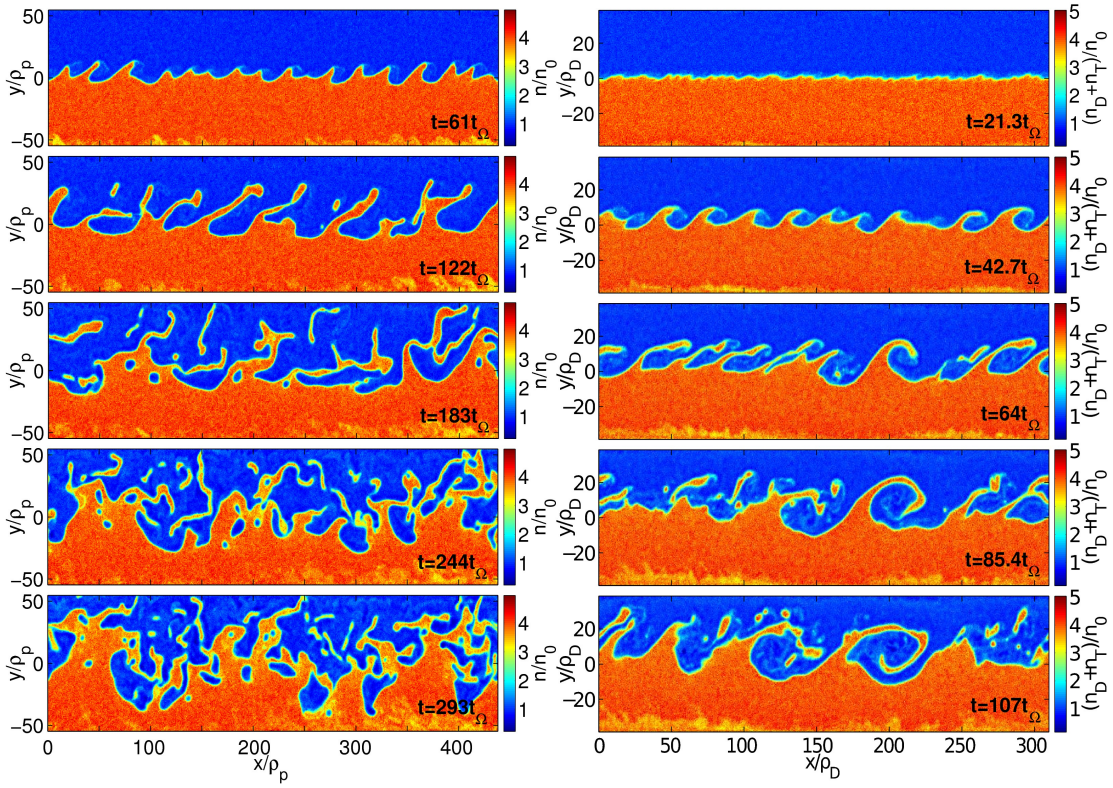

Fig.3 Total number density of ions for simulations of a proton plasma (left panels) and D-T plasma (right panels) initialised with a velocity shear boundary and pressure gradient at $y = 0$. The combination of K–H and interchange instabilities leads to separation of blobs significantly earlier than in the case with no shear boundary (Fig.2). Reproduced from [11].

ion gyro-scale blobs, and introduce a cut-off in the distribution function of blob sizes at small scales. The statistics of blob creation in proton compared to D–T plasmas imply that an increase of the ion gyro-radius results in an increase of the fraction of blobs at smaller scales. Analysis[11] of the mean square displacement of particles demonstrates that the ion kinetic interchange and Kelvin-Helmholtz instabilities lead to hyperdiffusion of particles in the radial direction, with diffusion power law exponent $\gamma \sim 2$–4. The introduction of a shear flow reduces this exponent, replicating experimental observations.

This work was part-funded by the RCUK Energy Programme and by the European Union's Horizon 2020 programme.

[1] A V Nedospasov, J. Nucl. Mater. **196** 90 (1992)
[2] M A Pedrosa M A *et al.*, Phys. Rev. Lett**. 82** 3621 (1999)
[3] S I Krasheninnikov, Phys. Lett. A **283** 368 (2001)
[4] S J Zweben *et al*., Plasma Phys. Control. Fusion **49** 1 (2007)
[5] J A Boedo *et al.*, Phys. Plasmas **8** 4826 (2001)
[6] O Grulke *et al.*, Phys. Plasmas **13** 012306 (2006)
[7] J R Myra *et al.*, Phys. Plasmas **13** 092509 (2006)
[8] B Nold *et al.*, Plasma Phys. Control. Fusion **52** 065005 (2010)
[9] A Kirk *et al.*, Plasma Phys. Control. Fusion **48** B433 (2006)
[10] A S Kukushkin *et al*., Nucl. Fusion **43** 716 (2003)
[11] P W Gingell *et al.*, Plasma Phys. Control Fusion **56** 035012 (2014)
[12] P W Gingell *et al.*, Plasma Phys. Control Fusion **54** 065005 (2012)
[13] P W Gingell *et al.*, Plasma Phys. Control Fusion **55** 055010 (2013)